

RAREFIED-FLOW AERODYNAMICS

FINAL SUMMARY REPORT

NASA Research Grant NAG-1-921

1 January 1989 to 31 May 1992

LANGLEY

GRANT

IN-02-CIR

104026

P-21

J. Leith Potter

Principal Investigator

(NASA-CR-190452) RAREFIED-FLOW AERODYNAMICS
Final Report, 1 Jan. 1989 - 31 May 1992
(Vanderbilt Univ.) 21 p

N92-27191

Unclas

G3/02 0104026

Vanderbilt University

Mechanical Engineering Department

P. O. Box 1592 Station B

Nashville, TN 37235

RAREFIED-FLOW AERODYNAMICS

This summary report concludes and documents research conducted under NASA Research Grant NAG-1-921. The principal results are described in three published papers (refs. 1-3) and in a fourth paper (ref. 4) which is to be presented at the 18th International Rarefied Gas Dynamics Symposium in July 1992. Abstracts of references 1-3 are reproduced in Appendix A of this report. Reference 4, not yet published, is included herein as Appendix B.

As the referenced publications show, one phase of this research has focused on means for relatively simple and quick procedures for estimating aerodynamic coefficients of lifting re-entry vehicles. The methods developed allow designers not only to evaluate the aerodynamics of specific shapes but also to optimize shapes under given constraints.

A second phase of work concerned the analysis of the effect of thermomolecular flow on pressures measured by an orifice near the nose of a Space Shuttle Orbiter at altitudes above 75 km. It was shown that pressures corrected for thermomolecular flow effect are in good agreement with values predicted by independent theoretical methods. An incidental product of this work was the insight gained regarding the free molecular thermal accommodation coefficient applicable under "real" conditions of high speed flow in the Earth's atmosphere.

REFERENCES

1. Potter, J. L. "Procedure for Estimating Aerodynamics of Three- Dimensional Bodies in Transitional Flow," *Progress in Astronautics and Aeronautics: Rarefied Gas Dynamics*, Vol. 118, ed. by E. P. Muntz, D. P. Weaver, and D. H. Campbell, AIAA, Washington, 1989, pp. 484-492.
2. Potter, J. L. and Blanchard, R. C. "Thermomolecular Effect on Pressure Measurements with Orifices in Transitional Flow," *Rarefied Gas Dynamics*, ed. by A. E. Beylich, VCH Verlagsgesellschaft mbH, Weinheim, 1991, pp. 1459-1465.
3. Potter, J. L. and Peterson, S. W. "Local Bridging to Predict Aerodynamic Coefficients in Hypersonic, Rarefied Flow," *Journal of Spacecraft and Rockets*, Vol. 29, No. 3, AIAA, Washington, May-June, 1992, pp. 344-351.
4. Potter, J. L. and Rockaway, J. K. "Aerodynamic Optimization for Hypersonic Flight at Very High Altitudes," to be presented at the 18th International Rarefied Gas Dynamics Symposium, Vancouver, B.C., 27-31 July 1992.

APPENDIX A

Abstracts of Published Work

Research Grant NAG-1-921

PROCEDURE FOR ESTIMATING AERODYNAMICS OF THREE-DIMENSIONAL BODIES IN TRANSITIONAL FLOW

ABSTRACT

Based on considerations of fluid dynamic simulation appropriate to hypersonic, viscous flow over blunt-nosed lifting bodies, a method was presented earlier by the author for estimating drag coefficients in the transitional-flow regime. The extension of the same method to prediction of lift coefficients is presented in this paper. Correlation of available experimental data by a simulation parameter appropriate for this purpose is the basis of the procedure described. Under low-density, hypersonic flow conditions, the overriding importance of projected and wetted areas, rather than details of body configuration, support this approach for finding aerodynamic forces. The ease of application of the method makes it useful for preliminary studies that involve a wide variety of three-dimensional vehicle configurations or a range of angles of attack of a given vehicle. It is also easy to examine the influence of different assumptions regarding gas/surface interaction parameters.

THERMOMOLECULAR EFFECT ON PRESSURE MEASUREMENTS WITH ORIFICES IN TRANSITIONAL FLOW

ABSTRACT

This study was undertaken to further evaluate a method for calculating the influence of thermomolecular flow upon pressures measured by means of orifices in walls exposed to rarefied gases. The last version of the method under discussion was developed over twenty years ago and presented at the 7th International RGD Symposium. At that time, no experimental pressure data for high-altitude re-entry flight were available. However, it has now become possible to examine the "orifice effect" under conditions significantly different from those for which the semiempirical (SE) method was earlier shown to be successful.

The lack of knowledge of the gas/surface interaction model to apply in a given case remains a major source of uncertainty in this and many other calculations of rarefied flows. Within the constraint imposed by that factor, it is shown that the SE correction gives acceptable results when used to predict surface pressure based on

measured internal pressure, or internal pressure based on theoretically predicted surface pressure. The implied energy accommodation coefficients appear to be plausible in all cases.

On the basis of comparisons between predicted results and both laboratory and flight data, plus limited DSMC calculations, it is suggested that the SE method remains a useful tool. It is relatively easy to apply and apparently gives good results if an appropriate energy accommodation coefficient is used.

LOCAL BRIDGING TO PREDICT AERODYNAMIC COEFFICIENTS IN HYPERSONIC, RAREFIED FLOW

ABSTRACT

A computational method is given for the prediction of local pressure and viscous shear stress on windward surfaces of convex, axisymmetric or quasi-axisymmetric, hypersonic bodies in the transitional, rarefied flow regime. Overall aerodynamic forces and moments are computed by integration of the local quantities. The method is based upon a correlation of local pressure and shear stress computed by the direct simulation Monte Carlo (DSMC) numerical technique for cold-wall, real gas conditions and some supplemental data from low-density, hypersonic wind tunnels. Two-dimensional shapes and leeward surfaces are not included in the scope of the method as it is presented here. Results are compared with DSMC and viscous shock layer (VSL) computations for both local and overall coefficients. Also included are sphere and blunt cone drag obtained from both computation and experiment, as well as lift and pitching moment coefficients for the NASA AFE vehicle at various angles of attack. It appears that the method presented here will prove adequate for relatively bluff bodies approximately defined by wetted length-to-nose radius ratios of less than ten.

APPENDIX B

Final Paper (Not Yet Published)

Research Grant NAG-1-921

AERODYNAMIC OPTIMIZATION FOR HYPERSONIC FLIGHT AT VERY HIGH ALTITUDES

**J. Leith Potter and J. Kent Rockaway
Department of Mechanical Engineering
Vanderbilt University
Nashville, TN 37235, U.S.A.**

Abstract

The advantages of an optimization approach to preliminary aerodynamic design of maneuvering aerospace vehicles and a method for doing that are demonstrated. An approximate method for estimating aerodynamic coefficients is linked to an optimization program for this purpose. Two waverider configurations are used as examples. It is shown that the greater potential for improved lift-to-drag ratio exists in the mid-transitional flow regime for the cases studied, and order-of-magnitude gains over bodies designed for lower altitude are predicted. An indication of the uncertainty in predictions of aerodynamic coefficients by the approximate method is provided by comparisons with experimental and Direct Simulation Monte Carlo results.

Nomenclature

C_D	= drag coefficient based on planform area
C_L	= lift coefficient based on planform area
C_N	= normal force coefficient based on planform area
D	= drag
H	= enthalpy
L	= lift
PFA	= projected frontal area

PPA	= projected planform area
Pn	= see Eq. (1)
s	= streamwise wetted length
s*	= see Eqs. (2-3)
U	= velocity
WA	= wetted area
ν	= kinematic viscosity

Subscripts

fm	= free-molecular flow
i	= inviscid flow
o	= freestream stagnation condition
w	= wall surface
∞	= freestream

Introduction

In early stages of aerodynamic design, it is often desirable to examine the effects of a large number of configuration and flight-condition variables. For that purpose, it will seldom be feasible to carry out elaborate computations or wind tunnel studies until a near-final design is selected. Approximate methods for predicting the overall aerodynamic coefficients must be relied on for screening or optimizing configurations. This paper illustrates the potential benefits of an optimization approach involving the linkage of a simple aerodynamic prediction method and an optimization code to find aerodynamic configurations that maximize lift-to-drag ratio (L/D) or other properties in rarefied flows. The advantage of higher L/D ratio for improved maneuverability or range of aerospace craft and the decrease in L/D at high altitudes and Mach numbers are well known to designers of such vehicles.

The method described in Refs. 1-2 is the basis for estimating aerodynamic coefficients. It is referred to as the Pn method hereafter, Pn being used as an abbreviation for "nth parameter." The optimization has been done by adapting an optimization program³ to the present purpose.

The aerodynamic shapes chosen for illustrating the results of optimization are of the "waverider" type.^{4, 5} This configuration has not previously been selected by designers of re-entry or aerobraking vehicles. This may be because pure waverider conditions require attached shock waves, i.e., sharp leading edges, limited angles of attack, and thin boundary layers. The waverider was invented to avoid the "spillage" or lateral flow that reduces pressures on 3-dimensional windward surfaces at large angles of incidence. An added benefit is that knowledge of the flow field of the hypothetical wedge or cone generating the flow field of the waverider simplifies aerodynamic analysis of the derived body. It is apparent that the basic waverider concept does not account for the blunt leading edges required for practical designs, nor the transitional rarefied flow phenomena that will affect the flow field, but the advantage of the waverider is not altogether lost when those less-than-ideal conditions exist.

Low-density, hypersonic flow involves thick shock and boundary layers and significant viscid-inviscid interaction at the lower Knudsen numbers of the transitional-flow regime. At higher Knudsen numbers, non-continuum phenomena are encountered. Therefore, it may seem inappropriate to use waverider configurations for studies concerning rarefied flow. However, the waverider is a suitable type of body for our analysis. The higher lift of the waverider, compared to flat bodies at equal conditions, recommends it for design of maneuvering re-entry vehicles when higher aerodynamic performance is needed. It simplifies the calculation of continuum, inviscid aerodynamic coefficients, and both leading edge bluntness and the loss of perfect waverider conditions in the transitional regime are accommodated by the Pn calculation method.

There is an issue regarding the concavity of the windward side of a waverider and the calculation of free-molecular flow in that region, i.e., can collisionless flow be assumed when some surface elements can "see" each other? That question has been discussed in Ref. 6 and, on the basis of that work, it is concluded that the concavity of the two configurations described later leads to errors of less than one percent when computing free-molecular aerodynamic coefficients.

Methods of Calculation

The Pn method is based upon a correlation of C_D and C_L data, mainly pertaining to lifting bodies, all at hypersonic Mach numbers.^{1, 2} The correlating parameter is defined as

$$Pn = \{ (U/v)_{\infty} s^* [H_{\infty} / (0.2 H_o + 0.5 H_w)]^{0.63} \}^{0.5} \dots \dots \dots (1)$$

For high-speed conditions, H_o is taken to be $U_{\infty}^2/2$. The modified wetted length, s^* , is defined differently for drag and lift calculations, so two forms of Pn are used. When C_D is sought,

$$s^* = s (PFA/ WA)^{0.5} \dots \dots \dots (2)$$

and Pn is denoted as Pn_D in this case. When C_L is sought,

$$s^* = s (PPA/ WA)^{0.5} \dots \dots \dots (3)$$

and the resulting Pn is denoted Pn_L . Normalized forms of C_D and C_L are defined as

$$\bar{C}_D = (C_D - C_{Di}) / (C_{Dfm} - C_{Di}) \dots \dots \dots (4)$$

$$\bar{C}_L = (C_L - C_{Li}) / (C_{Lfm} - C_{Li}) \dots \dots \dots (5)$$

and the correlated data are fitted by the functions

$$\bar{C}_D = [2.6 / (2.6 + Pn_D^{1.6})]^{0.5} \dots \dots \dots (6)$$

$$\overline{C}_L = [2.6/(2.6 + Pn_L^{1.6})]^{0.5} \dots\dots\dots (7)$$

The inviscid and free-molecular values of C_D and C_L are calculated by usual methods, e.g., modified Newtonian and fully accommodated, diffusely reflected free-molecular procedures, respectively.

Before discussing results of the optimization, it is necessary to examine the degree of agreement between the quick and approximate Pn method and experimental data or a more accurate, Direct Simulation Monte Carlo (DSMC) method. Such comparisons will give an appreciation of the approximation that may exist in the later optimization calculations.

The first example concerns a caret-delta model.⁷ This model was tested in the Imperial College gun tunnel at Mach number of 8.96, wall temperature of 295 K, total temperature of 1070 K, and unit Reynolds number of $1.22 \times 10^7/\text{m}$. Sweepback angle of the leading edge was 75 deg. Figure 1 shows the normal force coefficient, C_N , as a function of angle of attack, predicted by the Pn method and as measured. It is important to note that the shock would detach from a sharp wedge of approximately 44 deg at this Mach number, so the waverider quality of the model is lost at the higher angles of attack. This undoubtedly accounts for most of the divergence of the results above 40 deg, and we are reminded by this that other calculations for waveriders may become increasingly erroneous when very high angles of attack destroy the waverider property. Even under that condition, Coleman's⁷ data show the caret-delta producing greater C_N than the flat delta.

Figure 2 shows the results obtained for a 2-dimensional flat plate at 40-deg angle of attack. The DSMC data are from Ref. 8, and all conditions of the calculations were taken from that reference. A constant velocity of 7.5 km/s has been assumed, and Knudsen number is based on a flat plate wetted length of 12 m, corresponding to the mean aerodynamic chord of the Space Shuttle Orbiter. Real gas properties are taken into account. Surface temperatures vary from 1100 K at 100 km altitude to 175 K at 200 km. The maximum disagreement in L/D ratio is 20.9 percent of the DSMC value.

Figure 3 presents the comparison of Pn and DSMC methods as applied to the delta-wing wind tunnel model of Ref. 9. Because unheated hypersonic wind tunnel flow conditions are involved, wall-to-total temperature ratio is near 1.0, Mach number is 8.89, and Knudsen number is based on mean aerodynamic chord of the delta wing. Maximum disagreement in L/D ratio is 7.7 percent of the DSMC value. The results displayed in Figs. 1-3 are believed to justify use of the Pn method in performing the optimization study described hereafter.

The design optimization code, when linked to the design objective algorithm, computes the gradient of the objective with respect to the design variables. If constraints are imposed, gradients of the constraints are computed and the search direction takes account of gradients of the objective function and the constraints. As new values of the objective (maximum L/D) and the design variables are obtained, new gradients are computed, a new search direction is determined, and iterations continue until the optimum is found.

Conditions of Optimization and Results

Sketches of the two configurations of waveriders analyzed are shown in Fig. 4. The semi-cone has been required to have zero angle of attack, a volume of 2000 m^3 , a maximum length of 60 m, and a maximum angle β of 90 deg. The angle δ and radius R_b , as well as length s and angle β that yield maximum L/D have been found for flight conditions that correspond to a tethered satellite orbiting at altitudes of 80 to 130 km in the Earth's atmosphere. (See Table 1.) Wall temperature has been assumed constant at 350 K.

The caret-delta waverider in Fig. 4 is shown with zero thickness because only the windward surfaces are effective at the angles of attack (≥ 13.8 deg) that have been derived from the optimization. A fuselage of any shape could be contained within the lee flow of the wing without changing the computed lift and drag. In this case, the constant volume constraint has been replaced by a constant planform area constraint. Thus, a maximum length of 60 m, a planform area of 400 m^2 , and a value of 34.7 deg for η have been adopted.

The aerodynamic performance of the flat-topped half-cone configuration optimized to produce maximum L/D at each altitude is shown in Fig. 5. The corresponding semi-apex angle, δ , base radius, R_b , and axial length, s , are given in Fig. 6. The interrelation of pressure forces and shear forces, combined with the constraints on volume and length result in interesting changes in the optimum configuration for the various altitudes. The angle β , in every case, was found to be 90 deg, i.e., a full half-cone is indicated to be optimum for the conditions of the calculation. A number of other conditions and optimized qualities could be considered, but this example suffices to illustrate the guidance that can be provided for early design studies.

Aerodynamic results for the caret-delta configuration are presented in Fig. 7, and the corresponding angle of attack for optimum L/D is given in Fig. 8. Because of the requirement to maintain constant planform area and angle η , there is no variation in those quantities as altitude changes. In all cases, the maximum allowable length of 60 m is optimum, so a constant span is also indicated.

Recalling that diffuse reflection and full momentum accommodation have been assumed in these calculations, it is interesting to see the influence of E , the fraction of molecules reflected specularly. That assumption affects results at all altitudes because the P_n method is a transition-bridging method, with the free-molecular value of the aerodynamic coefficient providing a terminus or anchor point at infinite Knudsen number. Figure 9 illustrates the effect of E on maximum L/D of the optimized half-cone waveriders. Because of the effect of E on shear forces, L/D is improved with $0 < E \leq 1$.

Lift-to-drag ratios are small under the conditions studied, and it may seem unimportant to seek improvement. However, using the half-cone as an example, Fig. 10 shows the gain in L/D ratio when the body is optimized for each altitude. The results are normalized by the 80-km case, as though the configuration best for 80 km were also used at all higher altitudes. It is noteworthy that the greater gain occurs in the mid-transition range. A similar presenta-

tion for the caret-delta wing would show an advantage of slightly over 100 percent for the optimized configuration. Although other design considerations may dictate that the aerodynamically optimum shape not be chosen, knowledge of the optimum and the ability to optimize for a variety of constraints should be very helpful in preliminary design.

Acknowledgment

This work was supported by NASA Research Grant NAG-1-921, with R. C. Blanchard the cognizant Technical Officer. The authors are indebted to T. Ryder Booth for assistance in the research.

References

- ¹ Potter, J. L. "Transitional, Hypervelocity Aerodynamic Simulation and Scaling," *Progress in Astronautics and Aeronautics: Thermophysical Aspects of Re-Entry Flows*, Vol. 103, ed. by J. N. Moss and C. D. Scott, AIAA, New York, 1986, pp. 79-96.
- ² Potter, J. L. "Procedure for Estimating Aerodynamics of Three-Dimensional Bodies in Transitional Flow," *Progress in Astronautics and Aeronautics: Rarefied Gas Dynamics*, Vol. 118, ed. by E. P. Muntz, D. P. Weaver, and D. H. Campbell, AIAA, New York, 1989, pp. 484-492.
- ³ "Design Optimization Tools," a program licensed by VMA Engineering, 5960 Mandarin Ave., Suite F, Goleta, CA 93117.
- ⁴ Nonweiler, T. R., "Aerodynamic Problems of Manned Space Vehicles," *Journal of the Royal Aeronautical Society*, Vol. 63, 1959, pp. 521-528.
- ⁵ Townend, L. H., "Research and Design for Lifting Reentry," *Progress in Aerospace Sciences*, Vol. 18, Pergamon Press, New York, 1979, pp. 1-80.

- ⁶ Chahine, M. T., "Free-Molecule Flow Over Nonconvex Surfaces," *Rarefied Gas Dynamics, Advances in Applied Mechanics*, ed. by L. Talbot, Academic Press, New York, 1961, pp. 209-230.
- ⁷ Coleman, G. T., "Aerodynamic Force Measurement on Caret and Delta Wings at High Incidence," *Journal of Spacecraft and Rockets*, Vol. 10, No. 11, Nov. 1973, pp. 750-751.
- ⁸ Dogra, V. K. and Moss, J. N., "Hypersonic Rarefied Flow About Plates at Incidence," AIAA Paper 89-1712, June 1989.
- ⁹ Celenligil, C. and Moss, J. N., "Hypersonic Rarefied Flow About a Delta Wing — Direct Simulation and Comparison With Experiment," AIAA Paper 91-1315, June 1991.

Table 1. Flow Conditions

Altitude km =	80	90	100	110	120	125	130
U_{∞} km/s	7.61	7.62	7.63	7.65	7.66	7.67	7.67
$(U/v)_{\infty}$ 1/m	16040	2078	326	49.5	7.53	4.91	2.78
T_{∞} K	168	188	193	235	329	380	432

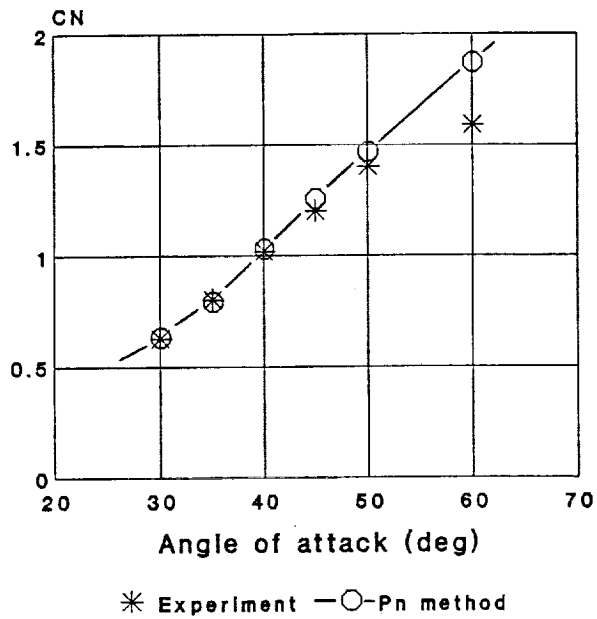


Fig. 1 Comparison of Pn method and experimental data of Ref. 7 for a caret-delta wing

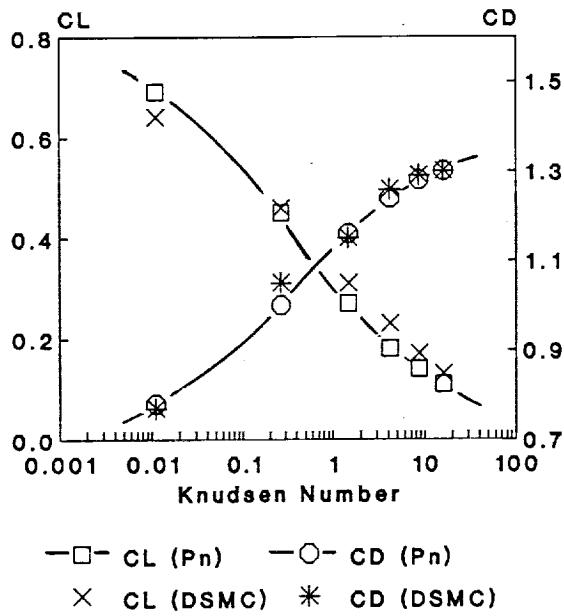


Fig. 2 Comparison of flat plate at 40 degree angle of attack. DSMC results from Ref. 8.

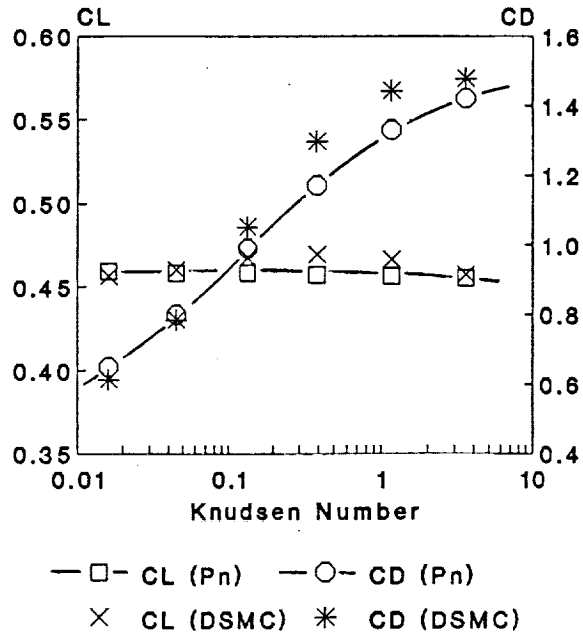


Fig. 3 Comparison of delta wing at 30 degree angle of attack. DSMC results from Ref. 9.

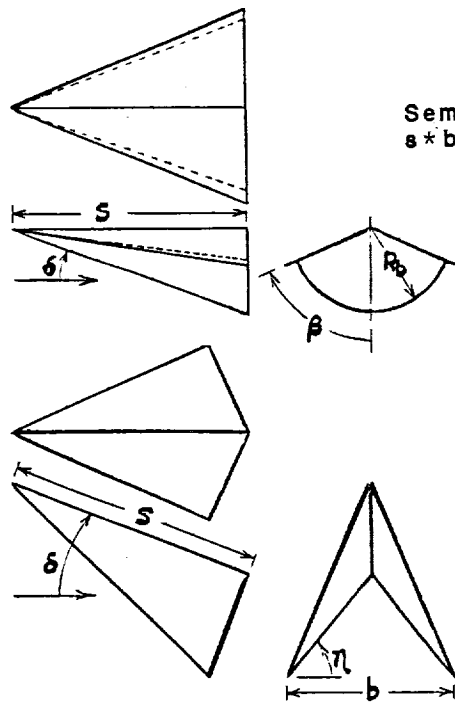


Fig. 4 Waverider configurations

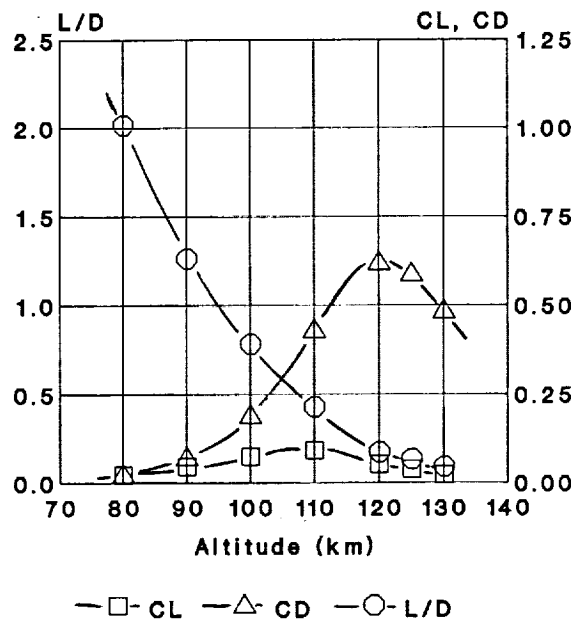


Fig. 5 Optimized half-cone waverider of constant volume at orbital speed. Results predicted by Pn method.

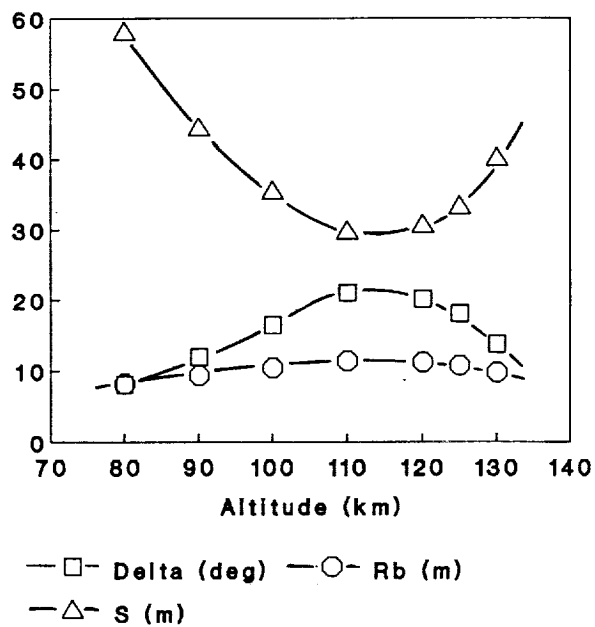


Fig. 6 Configurations of optimized conical waveriders. Results predicted by Pn method.

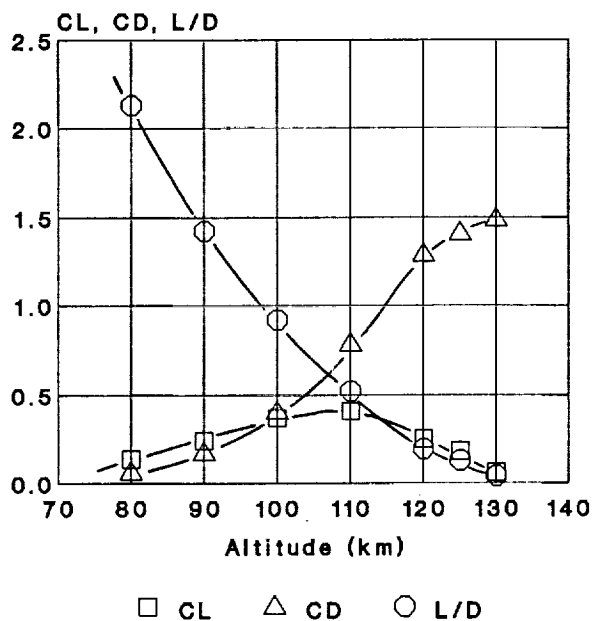


Fig. 7 Optimized caret-delta wing of constant planform area and zero thickness at orbital speed. Pn method.

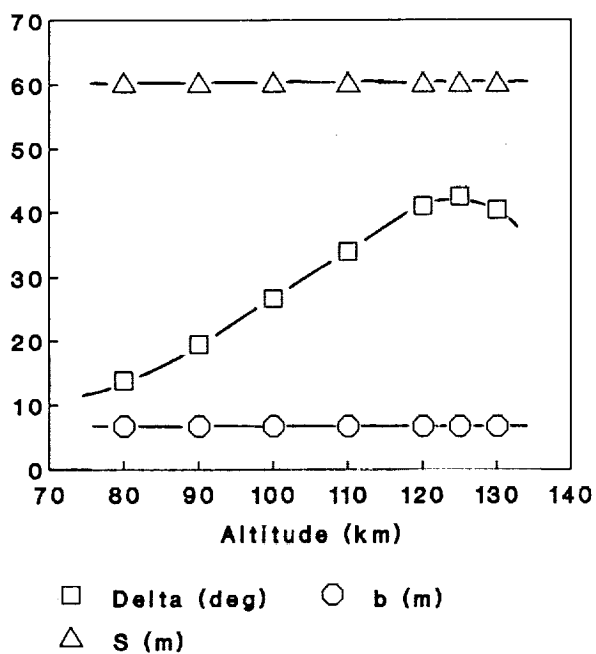


Fig. 8 Configurations of optimized caret-delta waveriders. Pn method.

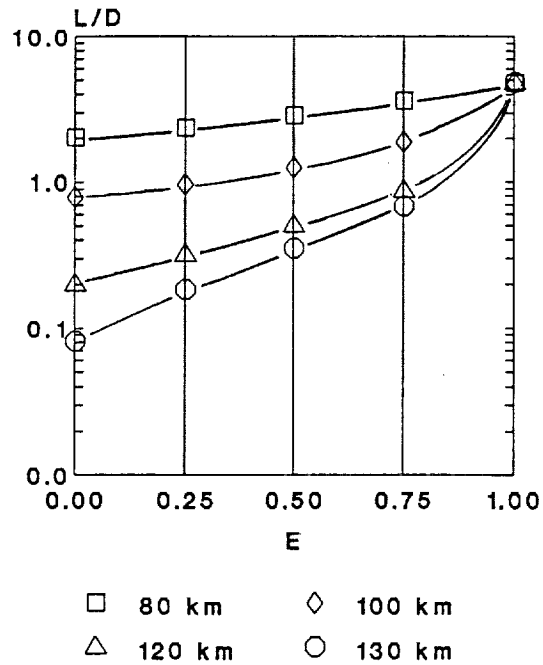


Fig. 9 Effect of E on lift-to-drag ratios for optimized half cones.

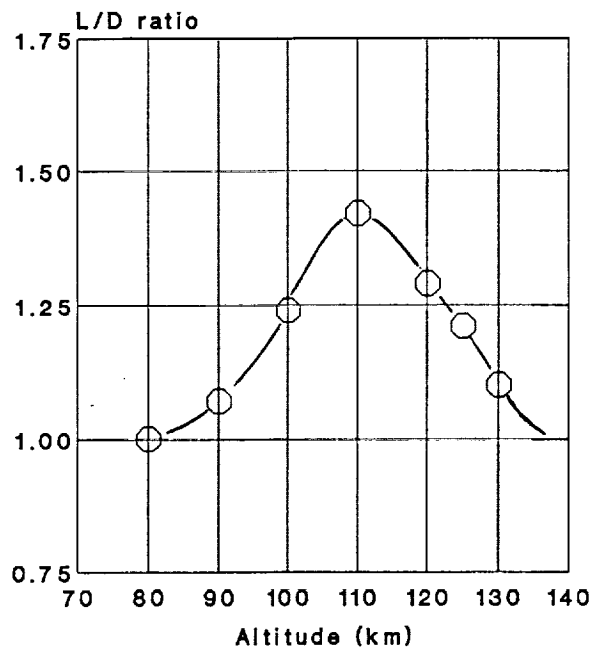


Fig. 10 Illustration of the advantage gained by optimizing the half-cone waverider for rarefied flow.